

THREE-DIMENSIONAL CONE-BEAM COMPUTED TOMOGRAPHY VOLUME  
REGISTRATION FOR THE ANALYSIS OF ALVEOLAR BONE CHANGES

Peter Thomas Green

A thesis submitted to the faculty at the University of North Carolina at Chapel Hill in partial fulfillment of the requirements for the degree of Master of Science in the School of Dentistry (Oral and Maxillofacial Radiology).

Chapel Hill  
2017

Approved by:

André Mol

Donald Tyndall

Antonio J. Moretti

Heidi Kohltfarber

© 2017  
Peter Thomas Green  
ALL RIGHTS RESERVED

## ABSTRACT

Peter Thomas Green: Three-dimensional Cone-Beam Computed Tomography Volume Registration for the Analysis of Alveolar Bone Changes  
(Under the direction of André Mol)

**Objectives:** 1. Determine accuracy of detecting bone loss affecting tooth support with registered cone-beam computed tomography (CBCT) compared to intraoral radiographs (IO). 2. Assess repeatability of measurements with CBCT compared to IO. 3. Identify factors which affect defect detection. 4. Determine effect of bucco-lingual bone thickness on defect detection.

**Methods:** Defects were created in mandibles and imaged pre-, post-defect with IO and CBCT. Six observers viewed IO radiographs pre-, post-defect followed by CBCTs to determine defect presence and extent. Receiver Operating Characteristic (ROC), sensitivity, specificity, logistic regression were used. Inter-, intra-observer agreement were assessed by intraclass correlation coefficient and weighted kappa. **Results:** Mean ROC  $A_z$  for CBCT (0.90) was not statistically different from mean  $A_z$  of IO (0.81). CBCT sensitivity was higher than IO sensitivity (0.85 vs. 0.63,  $p < 0.05$ ). CBCT specificity was equivalent to IO specificity (0.91 vs. 0.84,  $p > 0.05$ ). Bone thickness, imaging modality, observer had significant effects on bone loss detection. Odds ratio for CBCT vs. IO diagnostic accuracy was 2.29. Odds ratio for bucco-lingual bone thickness was 1.52. There was moderate agreement between observers and substantial agreement within observers for detection of bone loss and measurement of extent. **Conclusions:** CBCT showed equivalent diagnostic efficacy and specificity for defect detection, but higher sensitivity than IO. CBCT more than doubles the odds of accurate bone loss assessment compared to IO. Odds of bone loss detection increase approximately 50% per millimeter of bucco-lingual bone loss.

To my wife, Lauren Kelly Green.  
Without your love and support this would not be possible.

## **ACKNOWLEDGEMENTS**

Many people helped in this endeavor. A special thank you to my advisor Dr. André Mol and committee members Dr. Donald Tyndall, Dr. Antonio Moretti and Dr. Heidi Kohltharber. Without your guidance and patience this would not be possible. Thank you also to Dr. Ceib Phillips and Pooja Saha for their statistical support.

## TABLE OF CONTENTS

LIST OF FIGURES .....	vii
LIST OF TABLES .....	viii
LIST OF ABBREVIATIONS.....	ix
REVIEW OF THE LITERATURE .....	1
REFERENCES .....	8
MANUSCRIPT.....	11
Introduction.....	11
Materials and Methods.....	15
Results.....	20
Discussion.....	22
Conclusion .....	33
REFERENCES .....	35
APPENDIX I .....	46
APPENDIX II.....	47

## LIST OF FIGURES

Figure 1: Photograph of mandible with Play-Doh® soft tissue equivalent material .....	39
Figure 2: Intraoral radiographs pre- and post-defect .....	39
Figure 3: Measuring periodontal defect depth and bone width clinically .....	40
Figure 4: Superimposition windows with registered CBCTs .....	41
Figure 5: ROC curves based on pooled data between registered CBCTs and intraoral radiographs for detection of periodontal bone loss .....	42
Figure 6: Segmented mandibles pre- and post-defect in ITK-SNAP combined to show a color map of the same quadrant in 3D Slicer v. 3.1. ....	43
Figure 7: ROC curves for Observer 1 for Detection of Periodontal Bone defects with Intraoral Radiographs and Registered CBCTs.....	47
Figure 8: ROC curves for Observer 2 for Detection of Periodontal Bone defects with Intraoral Radiographs and Registered CBCTs.....	47
Figure 9: ROC curves for Observer 3 for Detection of Periodontal Bone defects with Intraoral Radiographs and Registered CBCTs.....	48
Figure 10: ROC curves for Observer 4 for Detection of Periodontal Bone defects with Intraoral Radiographs and Registered CBCTs.....	48
Figure 11: ROC curves for Observer 5 for Detection of Periodontal Bone defects with Intraoral Radiographs and Registered CBCTs.....	49
Figure 12: ROC curves for Observer 6 for Detection of Periodontal Bone defects with Intraoral Radiographs and Registered CBCTs.....	49

## LIST OF TABLES

Table 1: Periodontal Defect Ground Truth .....	44
Table 2: ROC area under the curve (AUC), sensitivity and specificity based on pooled data .....	44
Table 3: Paired t-tests for area under the curve (AUC), sensitivity and specificity between intraoral radiographs and registered CBCTs .....	44
Table 4: Type 3 Analysis of Effects .....	44
Table 5: Odds Ratio Estimates.....	44
Table 6: Inter-Observer Reliability (Intraclass Correlation).....	45
Table 7: Weighted Kappa Values for Confidence of Bone Loss Detection .....	45
Table 8: Weighted Kappa Values for Measurement of Bone Loss Extent .....	45
Table 9: Bowker's Test of Symmetry .....	45
Table 10: Individual ROC area under the curve (AUC), sensitivity and specificity data for each observer and imaging modality .....	46



## **LIST OF ABBREVIATIONS**

AM	Thesis Advisor (André Mol)
Az	Area under the ROC curve
CBCT	Cone Beam Computed Tomography
CCD	Charge-Coupled Device
DICOM	Digital Imaging and Communications in Medicine
ICC	Intraclass Correlation
IO	Intraoral Radiography
IRB	Institutional Review Board
kV	Kilovolt
mA	Milliamperage
MDCT	Multidetector Computed Tomography
PG	Peter Green (Primary Investigator)
PSP	Photostimulable Phosphor
ROC	Receiver Operating Characteristic (Curve)
SID	Source to Image-Receptor Distance
UNC	University of North Carolina at Chapel Hill

## **REVIEW OF THE LITERATURE**

Inflammation of the gingiva, or gingivitis, occurs due to a bacterial challenge. The bacterial biofilm which accumulates close to the gingival margin will initially illicit the recruitment of a non-specific immune response. As the biological insult progresses apically to the periodontium, the disease not only affects soft tissues, but begins to affect the alveolar bone as well. This destruction of hard tissue is part of a process known as periodontitis and leads to the demineralization and subsequent destruction of alveolar bone. This area is generally within a 2-mm radius around the root surfaces of teeth, but may progress beyond this limit.<sup>1</sup> Periodontitis has shown a predilection for areas where plaque accumulates and where it is difficult for patients to keep biofilm-free. One specific area is the posterior interproximal alveolar bone. This area is particularly susceptible to interdental craters which represent approximately two-thirds (62%) of all mandibular alveolar bone defects.<sup>2</sup> The prevalence of interproximal periodontal intrabony defects increases with age and has been found to occur slightly more frequently in males than females in some studies.<sup>3</sup>

The use of radiographs has long been part of both dental diagnosis and treatment planning due to their ability to assess the hard structures of the maxillofacial complex. Intraoral radiographs, which include bitewing and periapical radiography, are used in periodontics to assess periodontal bone support for the teeth. Intraoral imaging is easy to use, low cost, and provides remarkable anatomic detail.<sup>4</sup> However, a substantial amount of bone must be lost or demineralized (30-50%) before it is detected on a conventional intraoral radiograph.<sup>5-8</sup> Additionally, the main diagnostic task of assessing bone is limited to the interproximal alveolar

bone levels, as the teeth are superimposed on possible buccal or lingual defects.<sup>4</sup> This makes detection and measurement of 2-wall and 3-wall defects a diagnostic challenge as remaining bone may conceal the defects.<sup>4</sup> Despite the shortcomings previously noted, dentists still routinely assess two-dimensional intraoral radiographs for signs of progressing demineralization or pathologic change. This is typically achieved by comparing current radiographs to those taken at a previous appointment side by side on a computer monitor. Examining intraoral radiographs from two different appointments is not only limited because of the aforementioned reasons, it also requires a high level of standardization in the technique of image acquisition, which is difficult to attain under routine clinical conditions.

Digital subtraction radiography has proven useful in detecting changes in alveolar bone mineralization as low as 5%.<sup>9,10</sup> This technique requires two intraoral radiographs acquired at different time points with near-identical projection geometry and density. The two images are overlaid and processed to show exactly where bone resorption or bone deposition has taken place.<sup>11,12</sup> In addition to detecting alterations in alveolar bone height, digital subtraction radiography can also quantify changes in the bone density.<sup>13,14</sup> Digital subtraction radiography has also proven useful in assessing bone changes surrounding implants.<sup>11,12</sup> When projection geometry, image brightness and image contrast are adequately standardized, measurements made with digital subtraction radiography can be highly accurate. This technique has the potential to visualize other osseous changes seen with ridge resorption, as well as healing of periapical lesions and alveolar bone defects.

As with all imaging techniques, digital subtraction radiography is not without its inherent problems. The major limitations are twofold: (1) bone changes cannot be fully appreciated in all three dimensions resulting in incomplete assessment and (2) standardization of the projection

geometry and image density are difficult to achieve under clinical conditions. Therefore, this technique has not successfully transitioned from the research environment into clinical practice.

A possible solution to the limitations of digital subtraction radiography can be found in cone-beam computed tomography (CBCT). CBCT makes it possible to evaluate the maxillofacial complex in all three dimensions and provide three-dimensional volume reconstructions which can be viewed from any angle.<sup>15</sup> Furthermore, reconstructed slices allow visualization of the patient's trabecular bone in addition to cortical bone, thereby reducing "anatomic noise" so each anatomic structure can be assessed separately.<sup>16</sup> The use of serial CBCT scans to assess progression or regression of disease eliminates the requirement of having to standardize image acquisition geometry parameters as three-dimensional volumes can be reoriented without loss of their spatial integrity.

The use of two-dimensional conventional radiographs provides limited diagnostic value due to the superimposition of anatomical structures. This includes dental anatomy, but also the bone facial and lingual to a lesion. It has been documented that lesions are difficult to discern on two-dimensional intraoral radiographs when they are confined within the trabecular bone and do not reach or resorb the facial and lingual cortical plates.<sup>17,18</sup> This was later corroborated in additional research which included assessing the accuracy of CBCT, CCD (charge-coupled device) digital sensors and traditional film radiographs to detect periapical bone defects.<sup>19</sup> CBCT performed significantly better in terms of sensitivity and diagnostic accuracy compared to the digital and film-based two-dimensional radiographs. The authors attributed this difference to the defects being contained within trabecular bone and not involving the cortical plates. A similar study was carried out to compare the accuracy of CBCT and PSP plates to detect and quantify alveolar bone defects.<sup>20</sup> Defects were artificially created not only on mesial and distal surfaces,

but buccal and lingual to the teeth as well. The authors found that CBCT performed significantly better than PSP plates and were able to detect periodontal bone defects in all four areas surrounding the tooth.

While the superimposition of anatomic structures may cause difficulty in properly evaluating many aspects of a radiograph, it is especially true with the assessment of defects in the alveolar bone. Another study investigated CBCT and intraoral radiographs of alveolar bone defects, which were further categorized into furcation defects, one-, two-, or three-wall defects, fenestrations and dehiscences. It was found that CBCT was superior to intraoral radiographs for the detection of grade I furcation defects, three-wall defects, dehiscences and fenestrations.<sup>21</sup> These findings echo the sentiment by Mol in 2004, who stated that visualizing 3-wall defects is diagnostically difficult.<sup>4</sup> These findings are likely the result of the x-ray beam projecting through the walls of bone still present facial and lingual to the defect in the case of the grade I furcation defects and three-wall defects. Fenestrations and dehiscences would be difficult to assess due to thin cortical bone being superimposed over a dense root structure. One investigator arrived at different conclusions. After reviewing the literature, AlJehani came to the conclusion that while CBCT improved the visualization of bone defects and furcation defects, traditional intraoral radiographs were still superior in showing periodontal ligament spaces and bone quality. The authors concluded that CBCT does not offer an advantage over traditional intraoral radiographs for assessing alveolar bone levels.<sup>22</sup>

Regardless of the additional information received by viewing the alveolar bone in three-dimensions, there are still different philosophies as to the extent of its usefulness in periodontics. Two recent systematic reviews have reached slightly different conclusions in this regard. Walter and co-workers performed a systematic review of the literature, investigating reports of CBCT to

view the periodontium around maxillary and mandibular molars as well as vertical bone defects.<sup>23</sup> They found that CBCT was highly accurate in its ability to assess defect morphology as compared to periapical radiographs. This improvement in accuracy over periapical radiographs particularly increased when assessing maxillary molars, where CBCT was superior to periapical radiographs in detecting furcation defects.<sup>23</sup> The authors were careful to note that along with this increase in diagnostic capability comes increased radiation dose which should be considered prior to imaging and should not be recommended for routine assessment of alveolar bone defects.<sup>23</sup>

Nikolic-Jakoba and co-workers performed their systematic review concentrating on the different diagnostic efficacy levels for the use of CBCT in detection of intrabony and furcation defects.<sup>24</sup> Diagnostic imaging research focused on patient outcomes and, ultimately, societal benefit is the starting point from which healthcare communities may begin to accept these imaging modalities into their everyday patient care protocols. Fryback and Thornbury published their 6-tiered hierarchical model of efficacy in diagnostic imaging in 1991.<sup>25</sup> Level 1 pertains to technical efficacy such as spatial resolution, gray-scale, sharpness, etc. Level 2 pertains to diagnostic accuracy efficacy which includes studies calculating sensitivity, specificity and receiver operating characteristic (ROC) curves for the imaging modality. Level 3 is diagnostic thinking efficacy, which studies if a clinician's diagnosis changes with additional information provided by the new imaging modality as compared to using the standard imaging modality. Level 4 is therapeutic efficacy, which investigates the percentage of time where the clinician's treatment plan changed given the additional information. Another research question here is the number of times certain procedures would be avoided given the additional imaging information. Level 5 is patient outcome efficacy where the percentage of patients whose outcome improved

with the new diagnostic imaging is calculated as is their life expectancy. Level 6 focuses on societal efficacy and includes cost-effectiveness and cost-benefit analyses for the new imaging modality. Nikolic-Jakoba and co-workers found that, for 16 publications which investigated CBCT's use in assessing intrabony and furcation defects, only one study examined the societal efficacy (Level 6)<sup>26</sup>, one study examined diagnostic thinking efficacy (Level 3)<sup>27</sup>, and the rest examined diagnostic accuracy (Level 2). The systematic review concluded there was not enough evidence to support the use of CBCT for diagnosis and treatment planning of periodontal bone defects or furcation defects. Most of the studies were Level 2 and showed CBCT had higher diagnostic accuracy compared to both periapical radiographs and panoramic radiographs for showing periodontal bone defects and furcation defects. Therefore, although CBCT is highly accurate, more studies at levels other than 2 are necessary before CBCT can become part of the clinician's diagnostic workflow for assessing the periodontium.<sup>24</sup>

Despite the lack of research in levels other than diagnostic accuracy efficacy, there is still a relative lack of data concerning three-dimensional volume registrations and how it pertains to diagnosis and treatment planning, particularly in periodontal disease. In this study, it is proposed to visualize and quantify changes in bone as seen in periodontal disease by registering two CBCT volumes. By superimposing three-dimensional CBCT volumes, visualization and quantification of periodontal osseous changes in both jaws may be possible. The use of three-dimensional registration has shown to be an effective tool for post-operative assessment of changes in the temporomandibular joints, maxilla and mandible following orthognathic surgery.<sup>28-30</sup> With CBCT volume registration, it is not necessary to achieve identical patient positioning between acquisitions as it is with intraoral radiographs. With CBCT volumes, there is complete control of the image data. This means that perfect patient positioning is no longer

critical since the image data can be oriented post-acquisition by the user. By superimposing CBCT volumes, the location and extent of periodontal defects could be visualized in three dimensions. Digital subtraction radiography is highly accurate when strict parameters are followed, but three-dimensional volume registration may be highly accurate as well without the need for ideal patient positioning and beam angulation. Furthermore, the alveolar bone changes could be seen in all three dimensions and for all areas of the maxilla and mandible simultaneously. This information could provide a more accurate and comprehensive picture to clinicians and can have implications for multiple areas in dentistry.



## REFERENCES

1. Papapanou PN, Tonetti MS: Diagnosis and epidemiology of periodontal osseous lesions, *Periodontol 2000*. 2000;22:8.
2. Manson, JD, Nicholson, K. The Distribution of Bone Defects in Chronic Periodontitis. 1974. *J. Periodontol.* (45)2:88-92.
3. Wouters FR, Salonen LE, Helldén LB, Frithiof L. Prevalence of interproximal periodontal intrabony defects in an adult population in Sweden. A radiographic study. *J Clin Periodontol.* 1989;16:144.
4. Mol A. Imaging methods in periodontology. *Periodontol 2000*.2004;34:34-48.
5. Åkesson L, Håkansson J, Rohlin M. Comparison of panoramic and intraoral radiography and pocket probing for the measurement of the marginal bone level. *J Clin Periodontol.* 1992;19:326-332.
6. Eickholz P, Hausmann E. Accuracy of radiographic assessment of interproximal bone loss in intrabony defects using linear measurements. *Eur J Oral Sci.* 2000;108:70-73.
7. Pepelassi E, Diamanti-Kipioti A. Selection of the most accurate method of conventional radiography for the assessment of periodontal osseous destruction. *J Clin Periodontol.* 1997;24:557-567.
8. Tonetti M, Pini-Prato G, Williams R, Cortellini P. Periodontal regeneration of human infrabony defects: III. Diagnostic strategies to detect bone gain. *J Periodontol.* 1993;64:269-277.
9. Ortman LF, Dunford R, McHenry K, Hausmann E. Subtraction radiography and computer assisted densitometric analyses of standardized radiographs. A comparison study with <sup>125</sup>I absorptiometry. *J Periodontal Res.* 1985;20:644-651.
10. Reddy MS, Jeffcoat MK. Digital subtraction radiography. *Dent Clin North Am.* 1993;37:553-565.
11. Reddy MS, Jeffcoat MK. Methods of assessing periodontal regeneration. *Periodontol 2000*. 1999;19:87-103.
12. Jeffcoat M, Reddy M. Digital Subtraction Radiography for Longitudinal Assessment of Peri-Implant Bone Change: Method and Validation. *Adv Dent Res.* Aug, 1993;7(2):196-201.
13. Mol A, Dunn S. The performance of projective standardization for digital subtraction radiography. *Oral Surg Oral Med Oral Pathol Oral Radiol Endod.* 2003;96:373-382.
14. Mol A, Dunn SM. Effect of bone chip orientation on quantitative estimates of changes in bone mass using digital subtraction radiography. *J Periodontal Res.* 2003;38:296-302.

15. Ludlow JB, Davies-Ludlow LE, Brooks SL, Howerton WB. Dosimetry of 3 CBCT devices for oral and maxillofacial radiology: CB Mercuray, NewTom 3G and i-CAT. *Dentomaxillofac Radiol.* 2006;35:219-26.
16. Patel S. New dimensions in endodontic imaging: Part 2. Cone beam computed tomography. *International endodontic journal*, 2009. 42(6):463-475.
17. Bender I, Seltzer S. Roentgenographic and Direct Observation of Experimental Lesions in Bone: I. *Journal of Endodontics*, 2003. 29(11):702-706.
18. Bender I, Seltzer, S. Roentgenographic and Direct Observation of Experimental Lesions in Bone: II. *Journal of Endodontics*, 2003. 29(11):707-712.
19. Stavropoulos A, Wenzel A. Accuracy of cone beam dental CT, intraoral digital and conventional film radiography for the detection of periapical lesions. An ex vivo study in pig jaws. *Clinical Oral Investigations*, 2007. 11(1):101-106.
20. Mol A, Balasundaram A. In vitro cone beam computed tomography imaging of periodontal bone. *Dentomaxillofacial Radiology*. 2008;37:319-324.
21. Bayat S, Talaeipour A, Sarlati, F. Detection of simulated periodontal defects using cone-beam CT and digital intraoral radiography. *Dentomaxillofacial Radiology*. 2016;45,20160030.
22. AlJehani Y. Diagnostic Applications of Cone-Beam CT for Periodontal Diseases. *International Journal of Dentistry*. 2014. p. 1-5.
23. Walter C, Schmidt J, Dula K, Sculean A. Cone beam computed tomography (CBCT) for diagnosis and treatment planning in periodontology: A systematic review. *Quintessence Int.* 2016;47:25-37.
24. Nikolic-Jakoba N, Spin-Neto R, Wenzel A. Cone-Beam Computed Tomography for Detection of Intra-bony and Furcation Defects: A Systematic Review Based on a Hierarchical Model for Diagnostic Efficacy. *J Periodontol.* 2016;18(6):630-644.
25. Fryback D, Thornbury J. The efficacy of diagnostic imaging. *Med Decis Making* 1991;11:88-94.
26. Walter C, Weiger R, Dietrich T, Lang NP, Zitzmann NU. Does three-dimensional imaging offer a financial benefit for treating maxillary molars with furcation involvement? A pilot clinical case series. *Clin Oral Implants Res.* 2012;23:351-358.
27. Walter C, Kaner D, Berndt DC, Weiger R, Zitzmann NU. Three-dimensional imaging as a pre-operative tool in decision making for furcation surgery. *J Clin Periodontol.* 2009;36:250-257.

28. Cevidanes LH, Bailey LJ, Tucker SF, Styner MA, Mol A, Phillips CL, Proffit WR, Turvey T. Three-dimensional cone-beam computed tomography for assessment of mandibular changes after orthognathic surgery. *Am J Orthod Dentofacial Orthop*. 2007;131:44-50.
29. Carvalho F, Cevidanes L, Motta A, Almeida M, Phillips C. Three-dimensional assessment of mandibular advancement 1 year after surgery. *Am J Orthod Dentofacial Orthop*. 2010, April;137(4 Suppl).
30. Alhadidi A, Cevidanes LH, Paniagua B, Cook R, Festy F, Tyndall D. 3D quantification of mandibular asymmetry using the SPHARM-PDM tool box. *Int J Comput Assist Radiol Surg*. 2012, Mar;7(2):265-71.

## **MANUSCRIPT**

### **Introduction**

The level of alveolar bone may change throughout a patient's life. A decrease in bone levels can be caused by inflammatory processes. Likewise, an increase in bone levels can be the result of a reduction in inflammation. The periodontium is particularly susceptible to this waxing and waning of inflammatory mediators. Since as early as 1941 it has been shown that inflammatory mediators travel within vascular channels in the alveolar bone, particularly the trabecular bone.<sup>1,2</sup> Periodontal disease is pervasive with mild, moderate, and severe forms affecting one of every two adult Americans 30 years of age or older. This equates to approximately 47.2 percent or 64.7 million American adults. For adults 65 years of age and older that prevalence increases to 70.1 percent.<sup>3</sup> There are also additional comorbidities associated with periodontal disease, including diabetes and cardiovascular disease.<sup>3</sup>

A classification system was developed by Goldman and Cohen in 1958 to describe the morphological characteristics of alveolar bone defects.<sup>4</sup> A three-wall bone defect contains intact interproximal bone and facial and lingual walls. A two-wall bone defect has two of these three walls intact and one destroyed. For example, the buccal and lingual walls may be unaffected, but the proximal bone could be destroyed. One-wall bone defects contain only one wall with the other two walls destroyed. Many alveolar bone defects are not purely one-, two-, or three-wall defects. The apical part of the defect may have three walls, whereas the coronal aspect contains only one or two walls. These are known as combination defects.<sup>4</sup>

Dentists monitor alveolar bone levels with intraoral radiographs as an adjunctive diagnostic tool along with clinical examination and probing. However, this does not assess the bone defect in three dimensions and is not very sensitive for detecting demineralization of hard tissue. A substantial amount of bone loss or bone demineralization must be present (30-50%) before resorption is detected on a conventional intraoral radiograph.<sup>5-8</sup> Furthermore, the bucco-lingual width of the defect cannot be determined. Indeed, as noted by Goldman in 1958, “radiographic examination of the infrabony pocket discloses a vertical resorptive lesion but gives us no information concerning the base of the pocket.”<sup>4</sup> There is limited data regarding alveolar defect width and its visibility on intraoral radiographs. Two-dimensional imaging is also hindered by anatomic superimposition which may mask bone defects, particularly those which contain walls of bone buccal and lingual to the defect. Therefore, improved solutions for early detection are needed.

Digital subtraction radiography is a radiographic application that was first utilized in 1935 by Ziedses des Plantes.<sup>9</sup> Digital subtraction radiography has proven useful in detecting changes in alveolar bone mineralization as small as 5%.<sup>10,11</sup> In addition to detecting alterations in bone height, digital subtraction radiography can also quantify changes in the density of bone.<sup>12,13</sup> This radiographic technique has also proven useful in assessing bone changes surrounding implants.<sup>14,15</sup> To obtain a digital subtraction image requires two intraoral radiographs which are acquired at different points in time with near-identical projection geometry, image density and image contrast. The two images are overlaid and processed to cancel out structures that have remained the same and only show those areas where bone resorption or bone deposition has taken place.<sup>14,15</sup> The best subtraction results are obtained when the projection geometry and image density are reproduced exactly. However, there is a small margin of error allowable in

beam angulation change, which is approximately 6°. <sup>12</sup> While reproduction of the projection geometry and image density are the keystones which make digital subtraction radiography possible, they are also seen as its greatest limitation. <sup>9</sup> It takes time and effort to meet the requirements for successful digital subtraction imaging. Thus, the application of digital subtraction radiography in dentistry has been limited to research studies and is not being used in clinical practice.

Dentistry's newest imaging modality, cone-beam computed tomography (CBCT), provides a three-dimensional view of the maxillofacial complex. This has revolutionized the field of oral and maxillofacial radiology and the profession of dentistry. The practice of dental implant placement has benefited from three-dimensional imaging in its ability to assess patients' bone quantity in the treatment planning phase. Similar to digital subtraction radiography, CBCT has also proven useful in assessing bone loss surrounding implants. <sup>16</sup> As the spatial resolution of CBCT improves, we are now able to see anatomic structures in great detail. It has been shown that CBCT is able to provide improved visualization of the periodontal ligament space compared to traditional intraoral images. <sup>17</sup> Concerning alveolar bone loss, it has been shown that the healing of these defects is highly dependent upon defect anatomy, such as those contained within bone (three-wall) versus those which involve the facial or lingual cortical plates (two- or one-wall defects). Therefore, developing the surgical plan and choice of periodontal restorative materials which yield the most optimal outcome is predicated upon an accurate examination of defect anatomy. <sup>18</sup>

Recent advancements in CBCT software allow for three-dimensional assessment of bone changes over time which has implications for multiple areas of dentistry. This is achieved by registering CBCT scans, a process known as three-dimensional volume registration. This

registration creates an overlay of two scans which the clinician may view simultaneously, or the clinician may choose to toggle between the two scans. Viewing registered CBCT scans is similar to digital subtraction radiography in that it superimposes radiographic data, but without the need for exact reproduction of the projection geometry and with the added benefit of three-dimensional information. The technique of CBCT scan registration can be accomplished in a matter of minutes, making it a viable option in clinical practice. Little data exists on its effectiveness in monitoring alveolar bone changes. By superimposing two CBCT volumes from different time points, greater sensitivity in these changes may be obtained while being able to view those changes in three dimensions.

The purpose of the current study is to determine if registering CBCT scans allows for greater detection of changes in periodontal bone levels pre- and post-defect as compared to traditional two-dimensional intraoral radiographs. Within this purpose, there are four aims: 1. Determine the accuracy of detecting alveolar bone loss with registered CBCT scans compared to traditional two-dimensional intraoral radiographs. 2. Determine the repeatability of measurements with registered CBCT scans compared to intraoral radiographs. 3. Determine the factors which have a significant effect on bone loss detection in radiographs. 4. Determine the buccal-lingual bone thickness at which alveolar bone defects can be detected with intraoral radiographs. The null-hypothesis to be tested is that there is no difference in the accuracy, sensitivity or specificity for assessing alveolar bone levels between registered CBCT scans and intraoral radiographs.

## Materials and Methods

To test the hypothesis of this study, an *ex vivo* model was used in order to simulate as close as possible clinical conditions while controlling the actual changes of the specimens. Institutional review board (IRB) approval was obtained to collect de-identified, dried human mandibles and to carry out observation sessions at the University of North Carolina (UNC) at Chapel Hill School of Dentistry (IRB #: 15-1771). The study followed guidelines set forth by the Helsinki Declaration. Twenty-two mandibles previously acquired for another research project (IRB #: 14-3143) were collected. Due to the fact that the current project solely investigated alveolar bone levels in the posterior mandible in an *ex vivo* model, each mandible was assessed visually to determine the presence of molar and premolar teeth. Mandibles which were edentulous, containing only mandibular anterior teeth, containing teeth broken to the alveolar crest, or containing teeth with large metallic restorations which could induce metal artifacts in the CBCT scan, were excluded from the study. Following the exclusion process, a total of 14 mandibles were used for this study.

In order to simulate the attenuation characteristics of soft tissue, each mandible was covered with Play-Doh® at approximately 0.5 cm thickness around the alveolar bone, ascending ramus, and tongue space prior to pre- and post-defect imaging (Figure 1). This material has previously been used and shown that its attenuation characteristics closely resemble soft tissue radiographically.<sup>19</sup>

Each of the mandibles were imaged with a conventional imaging modality as well as with CBCT. In this study, photostimulable phosphor plates (PSP) (Gendex, Hatfield, PA) were used to represent the conventional imaging modality. A premolar and a molar periapical radiograph were acquired with a PSP plate for each quadrant (Figure 2A). Conventional radiographs were



acquired with a Focus x-ray source (Instrumentarium Dental, Tuusula, Finland) at 70 kVp, 8 mA, 0.32 s, at a 40 cm source to image-receptor distance (SID) using a rectangular collimator. The central x-ray beam was projected perpendicular to the teeth such that the alveolar bone between adjacent teeth could be adequately visualized. Imaging stents traditionally used in studies involving pre- and post-op radiographs were not used and care was taken to closely mimic the projection geometry between the pre- and post-op images. The reason for not using stents was the goal to mimic a typical clinical situation similar to previous studies.<sup>20</sup> As noted by Tsiklakis and co-workers, occlusal stents are used to make the projection geometry repeatable although they cannot eliminate rotation of the patient's head.<sup>21</sup> Additionally, use of the stents is not practical in routine clinical dentistry.<sup>21</sup> The exposed PSP plates were scanned in a ScanX IO ILE scanner (Air Techniques, Melville, NY) via the MiPACS Dental Enterprise Viewer 3.1.1401 operating ScanX Plugin Version 1.2.8 (Medicore Imaging, Charlotte, NC).

Following imaging with the conventional modality, pre-defect three-dimensional CBCT scans of each mandible were acquired using the Orthophos XG 3D CBCT unit with an 8 x 8 cm field of view (FOV) at 85 kV, 7 mA and 14.3 s (Dentsply Sirona, Inc., Long Island, NY, USA). Each mandible was placed on a round imaging platform which fit into the CBCT FOV. A foam block was used to raise the mandibles above the metallic platform to prevent metal artifacts. The CBCT volumes were exported as Digital Imaging and Communications in Medicine (DICOM) files from the Dentsply Sirona Sidexis software at a 0.3 mm voxel size. An isotropic voxel size of 0.3 mm has been shown to have the combined benefits of good diagnostic image quality and a low radiation dose.<sup>22-24</sup>

Potential sites for periodontal defects included the mesial and distal surfaces of each molar and premolar tooth. The potential sites were logged into a spreadsheet (Microsoft Excel

2013, Redmond, WA) and totaled 75 sites. A random number generator program in Microsoft Excel was used to determine which sites would serve as control sites (no bone loss) and which sites as experimental sites (periodontal bone defect). A total of 34 control sites and 41 experimental sites were identified for the purposes of this study. Bone defects were created in the experimental sites by an experienced periodontist using a diamond-tipped bur and air-driven handpiece. Each defect left the facial and lingual cortical plates intact. The defects were then measured with a UNC-15 periodontal probe to the deepest portion of the defect (Figure 3A). The ground truth of presence or absence of the created defects as well as their measured depths were recorded. The facial and lingual bone thickness of the walls surrounding the defects were then measured at the level of the crestal bone perpendicular to the cortical plates (Figure 3B). After creating the alveolar bone defects, the soft tissue equivalent material was readapted to the mandibles and a post-defect series of radiographs using PSP plates and a CBCT scan were acquired for each mandible (Figure 2B). The CBCT scans were registered with InVivo software (v. 5.4.5 Anatomage, San Jose, CA) using a combination of two registration techniques. Within the InVivo software, numerous landmarks were manually selected on the three-dimensionally rendered pre-defect mandible and those same landmarks were selected on the post-defect mandible. These points were then aligned which approximated both pre- and post-defect CBCT scans. This process was used to approximate the mandibles and is known as point-based registration. Surface-based registration, the second registration option with the InVivo software, was then used to automatically match the rendered surfaces of both pre- and post-defect mandibles to further minimize their distances.

Six observers were recruited to analyze the images. All observers had several years of training in oral and maxillofacial radiology and clinical experience to assess alveolar bone levels

on radiographs. Five of the observers were oral and maxillofacial radiology residents and one observer was a board certified oral and maxillofacial radiologist. The observers were given an orientation session regarding the purposes of the study, the definition of bone loss and various bone morphology characteristics, intraoral radiograph projection geometry, reason for registering two CBCT scans, how to register CBCT volumes, and proper use of a 5 point confidence rating scale. Informed consent from the observers was obtained prior to the orientation session.

Observers were asked to complete two diagnostic tasks. They were first asked to indicate their confidence regarding the presence or absence of alveolar bone loss between the time point 1 and time point 2 images using the following Likert scale: 1 = definitely no bone loss, 2 = probably no bone loss, 3 = unsure if bone loss is present or absent, 4 = bone loss probably present, 5 = bone loss definitely present. The observers were then asked to measure, in millimeters, the point of greatest defect depth using a five point ordinal scale where 1 = 0 mm, 2 = 0-2.4 mm, 3 = 2.5-4.9 mm, 4 = 5-7.4 mm, 5 = 7.5-10 mm. A depth score of 1 was assigned for cases when observers decided there was no bone loss present. The measurements were made with a distance measurement tool in MiPACS for the intraoral images and in InVivo v. 5.4.5 for the registered CBCT volumes. The observers recorded their answers in an anonymized score sheet. This process was completed for the intraoral radiographs followed by the registered CBCT volumes. All images and CBCT volumes were randomized and all observers viewed intraoral images first followed by the registered CBCT volumes.

Observers viewed time point 1 and time point 2 PSP radiographs simultaneously on dual monitor workstations with Lenovo LT2252p monitors (Lenovo, Beijing, China) using MiPACS Dental Enterprise Viewer 3.1.1401 software (Medicare Imaging, Charlotte, NC). The room was dimly lit to provide adequate viewing conditions. Registered CBCT volumes were examined

under the same ambient light conditions on a Lenovo W540 ThinkPad (Lenovo, Beijing, China) using the Superimposition feature of the InVivo software (Figure 4A and 4B). A TCG-18 test pattern quality control check was performed on each of the monitors prior to the observation sessions to ensure adequate brightness and contrast. The principal investigator was on site during all of the observation sessions to answer any questions that arose. After a washout period of 2-3 weeks, each observer viewed approximately half of the images a second time in order to calculate intra-observer reliability.

The observers' scores and ground truth data were used to create receiver operating characteristic (ROC) curves utilizing a web-based ROC analysis computer program from Johns Hopkins University School of Medicine ([www.jrocf.it.org](http://www.jrocf.it.org)). Area under the curve ( $A_z$ ) scores were obtained from the curves and sensitivity and specificity were calculated in Excel (Microsoft Excel 2013, Redmond, WA). For detection of periodontal bone loss presence, a response of 4 and 5 were considered to be correct. A response of 3 was considered a negative response since the observer was not able to come to a definitive diagnostic decision as to the presence and extent of periodontal disease. Intraclass correlation coefficients (ICC) were calculated as a measure of overall agreement between the six observers. Since there were six observers and multiple responses from each observer, the PROC MIXED program in SAS v. 9.4 software (SAS Institute, Inc. Cary, NC) was used to fit the data to a mixed linear model. A mixed linear model was used because it specified the complete probability distribution of the data using fixed-effects parameters and covariance parameters. This program is similar to ANOVA but more robust in that it can account for this mixture of fixed and random effects. The program performed a variance components analysis assessing the ratio of within image variability to between image variability. This was then used to estimate the overall inter-observer reliability for confidence of

bone loss detection and measurement of bone loss as well as imaging modality. For intra-observer agreement, linear weighted kappa values were computed for each observer as well as the Bowker's Test of Symmetry for discordances. Logistic regression was used to evaluate the effects of observers, imaging modalities, and buccal-lingual bone thickness. Intra-observer reliability and logistic regression were also completed using SAS v. 9.4 software. A  $p$ -value of  $<0.05$  was considered to be statistically significant.

## Results

A total of 75 sites were assessed in this study, 41 of which were experimental (defect) sites and 34 of which were control sites (Table 1). Regarding the detection of alveolar bone loss, the difference between the ROC  $A_z$  of CBCT ( $A_z = 0.90$ ) was not statistically different from the ROC  $A_z$  of intraoral radiographs ( $A_z = 0.81$ ) (Table 2 and Figure 5). Thus, the null-hypothesis of no difference between the two imaging modalities could not be rejected. CBCT did have a significantly higher sensitivity (0.85) compared to intraoral radiographs (0.63). The difference in specificity between CBCT and intraoral radiographs (0.91 and 0.85, respectively) was not statistically significant (Table 2). Paired t-tests were performed to determine the significance of the  $A_z$  values ( $p=0.059$ ), sensitivity ( $p=0.007$ ) and specificity ( $p=0.45$ ) between both imaging modalities (Table 3).

The bone thickness, imaging modality and observer all had a significant effect on the ability to detect and quantify bone loss ( $p<0.001$ ) (Table 4). Greater bucco-lingual bone thickness likely hid the defects especially when viewed on intraoral images. The imaging modality was likely significant in that viewing defects obscured by bone and dental anatomy was made possible with adjunctive three-dimensional views. Observers also had a significant effect

on visualizing bone loss because, regardless of the imaging modality used, the ability to diagnose bone defects is still dependent on an observer's individual diagnostic skill level. Type 3 Analysis of Effects showed a statistically significant difference in the detection of bone loss between the two imaging modalities when controlling for observer and bone thickness ( $p < 0.001$ ) (Table 4). Odds Ratio Estimates were 2.29 for CBCT vs. Intraoral and 1.52 for buccal-lingual bone thickness (Table 5). Therefore, CBCT had 2.29 times the odds of visualizing bone loss compared to intraoral radiographs. In regards to intraoral radiographs, for every 1 mm of bucco-lingual bone loss, the odds of visualizing bone loss increase by 1.52.

The inter-observer reliability for CBCT bone loss detection and defect size assessment, as measured by the intraclass correlation coefficient, was 0.59 and 0.56, respectively. For intraoral radiographs, the values were 0.56, and 0.58, respectively (Table 6). These results suggest an overall moderate agreement between the observers for bone loss detection and bone loss measurement. The average intra-observer agreement, as measured by weighted kappa values, was 0.62 for detection of bone loss in CBCT scans. CBCT intra-observer agreement for defect size was 0.62. Both values indicate substantial agreement (Tables 7 and 8). The intra-observer average weighted kappa value for detection of bone loss on intraoral radiographs was 0.52. Intra-observer agreement for defect size assessment on intraoral radiographs was 0.59. Both values indicate moderate intra-observer agreement for intraoral radiographs (Tables 7 and 8). Tests for Equal Kappa Coefficients were not significant for the majority of observers ( $p > 0.05$ ) (Tables 7 and 8). Bowker's Test of Symmetry was used to assess whether there was a systematic difference in the responses between the two viewing sessions for a given observer and imaging modality (Table 9). All values were greater than 0.05 suggesting all data was symmetrical and there were no differences between the two viewing sessions ( $p > 0.05$ ).

## Discussion

Osseous craters, a specific type of alveolar bone defect, are concavities of the alveolar crest in the interdental area which do not affect the facial and lingual cortical plates. These comprise about one-third of all alveolar bone defects and comprise approximately two-thirds (62%) of all mandibular alveolar bone defects.<sup>25,26</sup> Posterior interdental areas of the maxilla and mandible are challenging for patients to keep biofilm-free, which leads to an increased risk for persistent inflammation and consequent loss of alveolar bone. Pertaining specifically to the mandibular predilection, broad, flat architecture of the posterior interdental bone between mandibular molars may predispose the area to formation of an osseous crater. Craters are contained by the mandible's thick cortical plates which may preclude their discovery with intraoral radiographic examination. Additionally, the soft and hard tissue vasculature may easily allow the entrance of inflammatory factors.<sup>27-29</sup> Defects are classified based on the number of walls they have. Most defects in this category contain more walls in its apical portion (three walls) than its coronal portion (one or two walls).<sup>4</sup> The prevalence of these vertical, combined osseous defects increase with age.<sup>30</sup> In the current study, defects which did not penetrate the cortical plates were created. The reason for this was two-fold: (1) these defects are generally more difficult to detect radiographically because demineralization is difficult to ascertain prior to cortical plate involvement, and (2) one of the aims of the study was to determine the amount of bucco-lingual bone loss which must occur before defects are visualized with two-dimensional imaging.

The effect of the imaging modality on the ability of the observers to detect alveolar bone defects was assessed in two different ways. ROC analysis was used to determine diagnostic efficacy and logistic regression was used to determine which modality was more likely to

provide accurate results. Diagnostic efficacy was measured with receiver operating characteristic (ROC) curves, which is a widely accepted statistical method to compare efficacy in radiological studies.<sup>31-34</sup> ROC analysis is often used in assessing diagnostic imaging accuracy because it eliminates differences in the decision thresholds of the observers and thus removes observer bias. An ROC curve plots the observer's sensitivity (or true positive fraction) on the y-axis against the false positive fraction (one minus the specificity) on the x-axis. The response data from the observers consists of numerical responses based on a five-point Likert scale. This scale allows the observer to communicate whether they see or do not see a defect as well as their level of confidence. After grouping the response data according to a range of true positive and true negative cut-off levels, the observer's performance is plotted as points between representing the relationship between the false positive rate and the true positive rate. A line of best fit is created through these points which represents the ROC curve. It is the area under this curve ( $A_z$ ) which is a measure of diagnostic efficacy. Larger  $A_z$  values indicate higher diagnostic efficacy. Interpretation of  $A_z$  values generally can be made as follows:  $A_z$  of 1.0 is a perfect test,  $A_z$  of 0.9-0.99 is an excellent test,  $A_z$  of 0.8-0.89 is a good test,  $A_z$  of 0.7-0.79 is a fair test,  $A_z$  of 0.51-0.69 is a poor test and  $A_z$  of 0.5 is a useless test.<sup>35</sup>

While the ROC analysis provides a measure of diagnostic efficacy independent of the observers' decision threshold, it remains of interest to compute sensitivity and specificity as well. The trade-off between sensitivity and specificity is observer dependent and is determined by the each observer's decision threshold. The observer response data to construct the ROC curves can be used to compute sensitivity and specificity. For this purpose, the five-point Likert scale needs to be dichotomized. In this study, we considered a response of 3 (unsure) to be a negative response. While one could argue whether to consider this a negative or a positive response, we



believe that answering “unsure” for a diagnostic test indicates it does not sufficiently answer the diagnostic question and does not warrant a positive result. It is somewhat akin to a perfectly diagonal ROC curve with an  $A_z$  of 0.5, indicating that diagnosing presence or absence of disease is a coin toss.

The average  $A_z$  value for CBCT was larger than the average  $A_z$  value for intraoral radiographs, however, the difference was not statistically significant. A difference of 0.09 in the  $A_z$  values would be considered a clinically significant difference. The lack of statistical difference can be attributed to the relatively small number of observers and the variability between the observers. For observers 2 and 6, the difference between the modalities was only 0.01. The  $A_z$  value differences for the other four observers ranged from 0.06 to 0.25. It should also be noted that the average  $A_z$  value for intraoral was already good. This may have been the result of the way in which the defects were created or because of the controlled, benchtop conditions of this study which do not fully compare to a clinical setting. The level of expertise of the observers may also have contributed to this. The observers who participated in this study were first, second and third-year oral and maxillofacial graduate students as well as one board-certified oral and maxillofacial radiology faculty member. For example, observer 6 attained an  $A_z$  value for intraoral radiography of 0.91 and improved negligibly with CBCT. In comparing our results to a similar study, Mol and co-workers achieved CBCT mean  $A_z$  values of 0.82 and 0.79 for molars and premolars, respectively. Intraoral mean  $A_z$  values were 0.45 and 0.52 for molars and premolars, respectively.<sup>20</sup> The CBCT  $A_z$  values in the current study were possibly higher because a newer machine was used and image quality would likely improve after nearly a decade of industry development. The intraoral  $A_z$  values were higher in the current study possibly because there were no defects created buccal and lingual to the teeth, unlike the study

by Mol and co-workers. The current study did not include buccal or lingual defects because this would have likely yielded results biased in favor of CBCT. Had the current study decided to include buccal and lingual defects then the difference in  $A_z$  values between the two imaging modalities may have been statistically significant.

The difference in sensitivity between the two imaging modalities was statistically significant. Observers detected 85% of the lesions with CBCT and 63% of the lesions with intraoral radiographs. All observers showed better sensitivity with CBCT although not all to the same degree. The average difference in the specificity between the two modalities was 7% in favor of CBCT, but this difference was not statistically significant. Variability between the observers appears to be the main reason for the difference not being significant. For example, intraoral radiography had higher specificity than CBCT for observers 1 and 3 while specificity stayed the same for observer 6. Observer 5 on the other hand, had a specificity of 0.41 for intraoral radiography and 0.88 for CBCT. Based on these results, it can be assumed that failure to reject the null-hypothesis of no difference in diagnostic efficacy can be largely attributed to variability between the observers in specificity. This variability in inter-observer reliability is likely the reason for the high standard deviation, which reached 0.21 for specificity.

Another factor that may have compounded this issue is that the ROC  $A_z$  values were based on empirical curves, not fitted curves. In order to construct fitted ROC curves, observers must use the entire spectrum of the Likert scale. If this does not happen, the data is considered degenerate and an empirical curve is created rather than a fitted curve. Thus, ROC analysis works best if the observers are presented with a series of cases and controls that range in difficulty and if the observers are trained to match their response to their actual level of confidence. In this study, one observer had degenerate data for the first CBCT viewing session

and three observers had degenerate data for the second CBCT viewing session. In other words, the observers were less inclined to select each of the 5 responses and use the entire scale which would have generated fitted ROC curves. The degenerate data for CBCT can, to some degree, be explained by the fact that the diagnostic tasks were easier for the observers and, consequently, their level of confidence higher. While it was our original hope to generate fitted ROC curves, we viewed it as an unintended positive consequence that the entire scale was not used, indicating there was relative certainty as to the presence or absence of bone loss.

Logistic regression was utilized to examine how the two imaging modalities, bucco-lingual bone thickness, and observers were predictors of diagnostic efficacy. Logistic regression yielded a Type 3 Analysis of Effects and odds ratios. The Type 3 Analysis of Effects highlights that, while there may have been differences in diagnostic efficacy amongst observers, there was a statistically significant difference in the diagnostic efficacy between intraoral imaging and CBCT when controlling for the observer and bucco-lingual bone thickness. Therefore, the thickness of bone, the imaging modality, as well as the observer, all had a significant effect on the ability to detect bone loss.

Regarding the imaging modalities, the odds of making a correct decision for the presence or absence of bone loss with CBCT were 2.29 times greater than making such a decision with intraoral imaging. This finding substantiates the ability of three-dimensional CBCT imaging to show changes in bone architecture by displaying trabecular bone without superimposed cortical bone, ultimately leading to greater detection by the viewer. However, even with cortical plates concealing the lesions confined to trabecular bone, intraoral radiographs are the standard imaging modality for dentists to assess alveolar bone morphology. Regarding how bucco-lingual bone thickness affected defect visibility, for every 1 mm of trabecular bone loss in the buccal-

lingual dimension, the odds of detecting this defect increased 1.52 times when controlling for the imaging modality and observer. This finding is consistent with the notion that more buccolingual bone loss leads to less x-ray attenuation and therefore increased contrast between the defect and the unaffected bone. Unlike research highlighting the ability of intraoral radiographs to detect periapical lesions, an odds ratio for detecting periodontal bone loss with intraoral radiographs has not been published to our knowledge and further investigation is needed to corroborate this finding.

Inter-observer reliability values between the six observers for both imaging modalities indicated a moderate level of agreement for determining the presence or absence of bone loss as well as for determining the amount of bone loss. The intraclass correlation coefficients underscore the variation in accuracy, sensitivity, and specificity between the observers. Depending on the difficulty of the task, it can be expected that observers vary in their responses. The moderate agreement suggests that interpreting the images from the two imaging modalities were observer-specific as there was no substantial to perfect agreement. Due to the fact that there was no statistically significant difference in terms of agreement level between different observers, the two imaging modalities were deemed equivalent in terms of observer agreement.

The average intra-observer reliability, as measured by weighted kappa, was substantial for CBCT and moderate for intraoral radiography, both for determining the presence or absence of bone loss and for measurement of the defect size. Therefore, Tests for Equal Kappa Coefficients were used to see if there was a statistically significant difference between weighted kappa values for the two imaging modalities. For all observers, except one, there was no statistically significant difference between the weighted kappa values of the two imaging modalities, or rather, no significant difference in reliability between the two imaging modalities.

However, there was a statistically significant difference in the weighted kappa values between intraoral radiographs and registered CBCTs for observer 5. Weighted kappa values for observer 5 went from 0.22 and 0.29 for bone loss detection and measurement of bone loss extent on intraoral radiographs, respectively, to 0.70 and 0.78 for bone loss detection and measurement of bone loss extent on CBCT, respectively. This change in kappa values implies a change from fair agreement to substantial agreement. It seemed the added information of three-dimensional imaging helped in observer 5's consistency in deciding on lesion detection and extent. For lesion detection, this observer was an outlier in terms of specificity in intraoral radiography, which implies the observer was vulnerable to distractors mimicking bone loss. However, this finding could not be generalized to all observers. Observers 2 and 6 were more reliable with intraoral imaging than with CBCT, but these differences were not statistically significant. Given these data, it appears the reliability of intraoral radiography and CBCT was user dependent.

While we have demonstrated that viewing registering CBCT scans yields higher sensitivity and odds of visualizing bone loss compared to intraoral radiographs, there are still drawbacks for the serial acquisition of registered CBCTs for the sole purpose of assessing alveolar bone. The potential radiation burden associated with CBCT is the highest of the dental imaging modalities. It also takes additional time to process and register CBCT scans, a process that is not necessary when comparing intraoral radiographs. The technology still shows promise, however. Compared to a full mouth series, acquisition of a CBCT scan is more comfortable for the patient, requires less time to acquire, and is less technique sensitive. It is inherently simple to obtain an ideal, diagnostically acceptable CBCT scan, while several factors dependent on the operator, including projection geometry, are required for ideal intraoral radiographs. Furthermore, the development of low dose protocols is a current trend with CBCT

manufacturers. This would lower the risk of harmful effects from radiation, possibly justifying serial scans to be obtained to monitor a patient's periodontal health. Inevitable software and hardware improvements will undoubtedly lessen the time required for registering CBCT scans. Additional studies are warranted to see if there would be significant improvements between intraoral and three-dimensional imaging in detection for general dentists or periodontists. The comparison of registration accuracy based on exposure parameters (i.e. low dose versus higher dose) should also be investigated. Another avenue of exploration would be to examine the effectiveness of syncing and scrolling through two CBCT scans next to each other as seen in Dentsply Sirona's Sidexis 4 "Compare" feature, as opposed to registering and then viewing them superimposed. This scenario more closely resembles dentists comparing intraoral radiographs side by side.

Given these findings of registered CBCT scans compared to intraoral radiographs, there are additional applications of the three-dimensional data to aid in the dentist's diagnosis and treatment planning. Acquisition of three-dimensional image data has implications beyond viewing the data in axial, coronal, and sagittal planes. With improvements in computer processing and software algorithms, this data has now become the scaffold upon which new innovations in medical and dental imaging are built. Three-dimensional image data can be segmented to create surface renderings allowing for full visualization and 360° manipulation of the anatomical or pathological morphology. Segmentation has come to the forefront in medical modeling and is the basis for three-dimensional printing. Prior to the introduction of CBCT to the dental market, multi-detector computed tomography (MDCT) had already been used to generate three-dimensional models for use in surgery.<sup>36-38</sup> While MDCT historically has been the imaging modality from which to create hard tissue segmentations, CBCT has recently been shown to be

equivalent to MDCT in its ability to generate models.<sup>39</sup> Segmentation is now becoming a popular topic in dentistry and it is only a matter of time before it becomes as commonplace in dentistry as in medicine.

Segmented, surface-rendered models can be registered, similar to registering volume data from CBCT scans, allowing for further analysis. It allows radiologists and clinicians to both calculate and visualize the estimated volume of change between the two segmentations. This has been used in multiple areas of dentistry including the diagnosis of developmental conditions such as mandibular asymmetry, degenerative changes associated with the temporomandibular joint, and mandibular bone changes following orthognathic surgery.<sup>19,40,41</sup> The technology extends beyond radiological imaging studies which use ionizing radiation. Surface renderings created by optical scan data can also be registered for use in dental education. Intraoral optical scans of a student's waxed crown or crown preparation can be registered to the faculty's gold standard crown and distance thresholds are chosen to generate a final grade.<sup>42,43</sup> Discrepancies in distance create a colored surface rendering to let students know where they under- or over-reduced their tooth, allowing them instant feedback for how and where to improve their preparations. Students found this objective method of grading preferable to subjective hand-grading.<sup>44</sup>

Software is currently available for segmentation and three-dimensional volume registration. In the context of the current study, these software programs may allow the oral and maxillofacial radiologist to both calculate and visualize the estimated volume of alveolar bone lost around teeth. To illustrate this technique, ITK-SNAP v.2.4 software was used for semi-automatic segmentation of the CBCT volumes. Three-dimensional surface renderings were created of the scan of the pre-defect dried mandible as well as of the scan of the post-defect dried mandible (Figures 6A and 6B) ([www.itksnap.org](http://www.itksnap.org)).<sup>45</sup> These segmented surface renderings were

then registered using 3D Slicer v. 3.1 software with a combination of fiducial registration, surface registration, and fine-tuned with region of interest (ROI) registration (www.slicer.org).<sup>46,47</sup> To localize and quantify the absolute distance of these changes between the two time points, the Shape Analysis: Model to Model Distance and Shape Population Viewer Modules were used to create a color-coded registration of the segmented data, also known as a color map (Figure 6C). Areas colored green indicated no change in bone morphology, red indicated an inward change in bone morphology (bone loss), blue indicated an outward change in bone morphology (bone gain).

The overarching goal of the current study was to develop a method by which CBCT can be used to more accurately and reliably detect and quantify changes in alveolar bone over time. Developing a method for creating a three-dimensional volume or surface registration has the potential to provide a complete visualization of the periodontal defects in a format that the clinician can readily appreciate. From a clinical perspective, it is critical that this protocol is able to be performed efficiently and accurately. The future implications for this are far reaching. While three-dimensional volume registration is already being used in the post-operative assessment of orthognathic surgery which requires a large field of view scan, this diagnostic procedure has numerous other implications. The methodology could be applied to investigate bone demineralization and trabecular bone density *in vivo*. Analysis of the density and organization of trabecular bone could be achieved with the data obtained from the three-dimensional models. Following creation of these three-dimensional models, a range could be created from the histogram of the CBCT volumes whereby the voxels in each area of interest would be classified as either trabecular bone or marrow space. This would help determine the density of trabeculation in the areas of interest.



Furthermore, three-dimensional volume registration has other dental applications which could include implant site assessment, root resorption detection, and assessment of impacted teeth. These diagnostic questions would allow for a small field of view setting with CBCT, which would make assessment of individual areas of interest more feasible. The efficiency and accuracy of three-dimensional volume registration to view alveolar bone loss, combined with the ability to show the referring clinician a color-coded topographical map depicting the extent of bone change, as well as its change in density, has the potential to be a useful method of radiological assessment.

There are a number of potential limitations of the current study. Due to the fact that metal artifact is an issue in CBCT imaging, mandibles which contained teeth with large metallic restorations were excluded from the study. It can be hypothesized that the effect of metal artifacts may be minimal as most of these artifacts are generated in the direction of the beam and therefore largely propagate in the axial plane above the crestal bone. It is possible, however, that metal artifacts would have predisposed the registration of CBCT volumes to error. Any large error in registration would create inaccurate detection and measurement of bone defects between the two CBCT scans during the observer sessions. In clinical practice, many older patients with periodontal disease are likely to have more restorations, some of which will be metallic.

Unbeknownst to the participating observers, no defects were created which measured 0-2.4 mm. This was because a connective tissue attachment of approximately 2 mm exists between the most inferior portion of a periodontal pocket and the most inferior portion of a periodontal bone defect.<sup>30</sup> Defect depths of less than 2 mm may actually not extend apically to the level of the alveolar crest and would not be considered intrabony defects; therefore, these were not used in the current study. Furthermore, only mandibles were used for this study due to their utilization

in a previous research project. Having maxillary dentition would have made the study more clinically relevant.

The angle of a periodontal bone defect has been shown to play a role in treatment prognosis. An angle of less than 45° between the root and side of the defect has been associated with a higher chance of success for regaining bone.<sup>48</sup> However, the current study was solely concerned with comparing defect detection and defect depth assessment between two imaging modalities rather than assessing treatment outcomes and observers were not tasked with measuring defect angles. Lastly, the method used for registration of the CBCT scans was a combination of point-based registration and surface-based registration. In the hierarchy of accuracy for aligning three-dimensional volumes, voxel-based registration is superior, allowing for superimposition of two volumes at the level of voxels, the three-dimensional version of a pixel. Surface-based registration allows for the automatic alignment of three-dimensional volumes based on the shape. Point-based registration is the least accurate, where the operator manually selects points on both images, and the images align based on those points. While voxel-based registration allows for slightly less variability in registration, surface-to-surface registration has been proven successful in previous studies and is within an acceptable level of accuracy without any statistically significant difference from voxel-based registration.<sup>49</sup>

## **Conclusion**

In the current study, registered CBCTs on average were not statistically significant in terms of diagnostic efficacy accuracy or specificity when compared to intraoral radiography. Registered CBCTs on average were shown to be statistically significantly more sensitive compared to intraoral radiographs. Registered CBCTs and intraoral radiographs showed

moderate agreement between observers. Registered CBCTs and intraoral radiographs showed substantial and moderate agreement within observers, respectively. No significant differences in reliability were found between the two imaging modalities except for one observer. These findings suggest that while registered CBCTs proved more sensitive, assessing alveolar bone loss is user-specific. Furthermore, our results suggest that specific to intraoral radiography, for every 1 mm of bone lost in the bucco-lingual dimension, the odds of detecting those defects increases by 1.52 times. To our knowledge, the odds of detecting alveolar bone loss with intraoral radiographs has not yet been published and further investigation is needed. Finally, we have shown it is possible to manipulate CBCT scans with segmentation and registration software to create three-dimensional dynamic data sets known as color maps that may help the clinician determine the location and extent of alveolar bone loss.

## REFERENCES

1. Weinmann JP. Progress of gingival inflammation into the supporting structures of the teeth. *J Periodont*. July 1941. 12:71.
2. Goldman HM. Extension of Exudate into Supporting Structures of the Teeth in Marginal Periodontics. *J. Periodont*. July 1957. 28:175.
3. Eke P, Dye B, Wei L, Thornton-Evans G, Genco R. Prevalence of Periodontitis in Adults in the United States: 2009 and 2010. *J Dent Res*. Aug, 2012. 91(10):914-920.
4. Goldman HM, Cohen DW. The infrabony pocket: classification and treatment, *J Periodontol*. Oct 1958. 29(4):272-291.
5. Åkesson L, Håkansson J, Rohlin M. Comparison of panoramic and intraoral radiography and pocket probing for the measurement of the marginal bone level. *J Clin Periodontol*. 1992;19:326-332.
6. Eickholz P, Hausmann E. Accuracy of radiographic assessment of interproximal bone loss in intrabony defects using linear measurements. *Eur J Oral Sci*. 2000;108:70-73.
7. Pepelassi E, Diamanti-Kipioti A. Selection of the most accurate method of conventional radiography for the assessment of periodontal osseous destruction. *J Clin Periodontol*. 1997;24:557-567.
8. Tonetti M, Pini-Prato G, Williams R, Cortellini P. Periodontal regeneration of human infrabony defects: III. Diagnostic strategies to detect bone gain. *J Periodontol*. 1993;64:269-277.
9. Mol A. Imaging methods in periodontology. *Periodontol 2000*. 2004;34:34-48.
10. Ortman LF, Dunford R, McHenry K, Hausmann E. Subtraction radiography and computer assisted densitometric analyses of standardized radiographs. A comparison study with <sup>125</sup>I absorptiometry. *J Periodontal Res*. 1985;20:644-651.
11. Reddy MS, Jeffcoat MK. Digital subtraction radiography. *Dent Clin North Am*. 1993;37:553-565.
12. Mol A, Dunn SM. The performance of projective standardization for digital subtraction radiography. *Oral Surg Oral Med Oral Pathol Oral Radiol Endod*. 2003;96:373-382.
13. Mol A, Dunn SM. Effect of bone chip orientation on quantitative estimates of changes in bone mass using digital subtraction radiography. *J Periodontal Res*. 2003;38:296-302.
14. Reddy MS, Jeffcoat MK. Methods of assessing periodontal regeneration. *Periodontol 2000*. 1999;19:87-103.

15. Jeffcoat MK, Reddy MS. *Digital Subtraction Radiography for Longitudinal Assessment of Peri-Implant Bone Change: Method and Validation*. *Adv Dent Res*. Aug, 1993;7(2):196-201.
16. Yepes J, Al-Sabbagh M. Use of Cone-Beam Computed Tomography in Early Detection of Implant Failure. *Dent Clin N Am*. 2015;59:41-56.
17. Jervøe-Storm P, Hagner M, Neugebauer J, Ritter L, Zöller J, Jepsen S, Frentzen M. Comparison of cone-beam computerized tomography and intraoral radiographs for determination of the periodontal ligament in a variable phantom. *Oral Surg Oral Med Oral Pathol Oral Radiol Endod*. 2010;109:e95-e101.
18. Hägi T, Laugisch O, Ivanovic A, Sculean A. Regenerative periodontal therapy. *Quintessence Int*. 2014;45:185-192.
19. Kohltfarber HB, Festy F, Alhadidi A, Tyndall D. Validation of 3D Surface Models of the Mandibular Condyles. Department of Diagnostic Sciences, UNC School of Dentistry; King's College London; The University of Jordan, Department of Diagnostic Sciences. *2016 American Academy of Oral and Maxillofacial Radiology Annual Session*. 29 Sept 2016. Scottsdale, AZ.
20. Bayat S, Talaeipour A, Sarlati F. Detection of simulated periodontal defects using cone-beam CT and digital intraoral radiography. *Dentomaxillofacial Radiology*. 2016; 45, 20160030.
21. Tsiklakis K, Paraschis A, van der Stelt PF. Projective reconstruction of non-standardized radiographs in digital subtraction radiography. *Dentomaxillofacial Radiology*. 1995;24(2):105-106.
22. Waltrick KB, Nunes de Abreu MJ Junior, Correa M, Zastrow MD, Dutra VD. Accuracy of linear measurements and visibility of the mandibular canal of cone-beam computed tomography images with different voxel sizes: An in vitro study. *J Periodontol*. 2013;84:68-77.
23. Hekmatian E, Jafari-Pozve N, Khorrami L. The effect of voxel size on the measurement of mandibular thickness in cone-beam computed tomography. *Dent Res J (Isfahan)*. 2014;11:544-548.
24. Patel A, Tee BC, Fields H, et al. Evaluation of cone-beam computed tomography in the diagnosis of simulated small osseous defects in the mandibular condyle. *AM J Orthod Dentofacial Orthop*. 2014;145:143-156.
25. Masters DH, Hoskins SW. Projection of cervical enamel into molar furcations. *J Periodontol*. 35:49, 1963.
26. Melcher AH, Eastoe JE: Biology of the periodontium. New York, 1969, Academic Press.
27. Manson JD. Bone morphology and bone loss in periodontal disease. *J Clin Periodontol*. 3:14, 1976.

28. Manson JD, Nicholson K. The distribution of bone defects in chronic periodontitis. *J Periodontol.* 45:88, 1974.
29. Nery EB, Corn H, Eisenstein IL. Palatal exostoses in the molar region. *J Periodontol.* 48:663, 1977.
30. Nielsen JJ, Glavind L, Karring T. Interproximal periodontal intrabony defects: prevalence, localization and etiological factors. *J Clin Periodontol.* 7:187, 1980.
31. Metz CE. Basic principles of ROC analysis. *Seminars in nuclear medicine.* Oct 1978;8(4):283-298.
32. Metz CE. ROC methodology in radiologic imaging. *Invest Radiol.* 1986;21:720-733.
33. Metz CE. ROC analysis in medical imaging: a tutorial review of the literature. *Radiological physics and technology.* Jan 2008;1(1):2-12.
34. van Erkel AR, Pattynama PM. Receiver operating characteristic (ROC) analysis: basic principles and applications in radiology. *European journal of radiology.* May 1998;27(2):88-94.
35. Ebell M. 4.6: Receiver Operating Characteristic Curves. Chapter 4 - Diagnosis I. Evidence-Based Practice for the Health Professions. *Institute for Evidence-Based Health Professions Education at the University of Georgia College of Public Health.* Accessed September 2016. <<http://ebp.uga.edu/courses/>>.
36. Mercuri LG., Wolford LM, Sanders B, White RD, Hurder A, Henderson W. Custom CAD/CAM total temporomandibular joint reconstruction system: preliminary multicenter report. *J Oral Maxillofac Surg.* 1995;53:106-115.
37. Wolford LM, Pitta MC, Reiche-Fischel O, Franco PF. TMJ Concepts/Techmedica custom-made TMJ total joint prosthesis: 5-year follow-up study. *Int J Oral Maxillofac Surg.* 2003;32:268-274.
38. Guarda-Nardini L, Manfredini D, Ferronato G. Temporomandibular joint total replacement prosthesis: Current knowledge and considerations for the future. *Int J Oral Maxillofac Surg.* 2008;37:103-110.
39. Gomes L, Gomes M, Gonçalves J, Ruellas A, Wolford L, Paniagua B, Benavides E, Cevidanes L. Cone beam computed tomography-based models versus multislice spiral computed tomography-based models for assessing condylar morphology. *Oral Surg Oral Med Oral Pathol Oral Radiol.* 2016;121:96-105.
40. Cevidanes LH, Bailey LJ, Tucker SF, Styner MA, Mol A, Phillips CL, Proffit WR, Turvey T. Three-dimensional cone-beam computed tomography for assessment of mandibular changes after orthognathic surgery. *Am J Orthod Dentofacial Orthop* 2007; 131: 44-50.

41. Alhadidi A, Cevidanes LH, Paniagua B, Cook R, Festy F, Tyndall D. 3D quantification of mandibular asymmetry using the SPHARM-PDM tool box. *Int J Comput Assist Radiol Surg* 2012 Mar;7(2):265-71.
42. Renne W, McGill ST, Mennito A, Wolf B, Marlow N, Shaftman S, Holmes JR. E4D Compare Software: An Alternative to Faculty Grading in Dental Education. *Journal of Dental Education*. 2013, Feb. 77(2). 168-175.
43. McPherson K, Mennito A, Vuthiganon J, Kritzas Y, McKinney R, Wolf B, Renne W. Utilizing Self-Assessment Software to Evaluate Student Wax-Ups in Dental Morphology. *Journal of Dental Education*. 2015, Jun. 79(6). 697-704.
44. Hamil L, Mennito A, Renne W, Vuthiganon J. Dental Students' Opinions of Preparation Assessment with E4D Compare Software Versus Traditional Methods. *Journal of Dental Education*. 2014, Oct. 78(10): 1424-1431.
45. Yushkevich PA, Piven J, Hazlett HC, Smith RG, Ho S, Gee JC, Gerig G. User-guided 3D active contour segmentation of anatomical structures: Significantly improved efficiency and reliability. *Neuroimage* 2006 Jul 1;31(3):1116-28.
46. Pieper S, Halle M, Kikinis R. 3D SLICER. *Proceedings of the 1st IEEE International Symposium on Biomedical Imaging: From Nano to Macro 2004*; 1:632-635.
47. Pieper S, Lorensen B, Schroeder W, Kikinis R. The NA-MIC Kit: ITK, VTK, Pipelines, Grids and 3D Slicer as an Open Platform for the Medical Image Computing Community. *Proceedings of the 3rd IEEE International Symposium on Biomedical Imaging: From Nano to Macro 2006*; 1:698-701.
48. Steffensen B, Weber HP. Relationship Between the Radiographic Periodontal Defect Angle and Healing After Treatment. *Journal of Periodontology*. 1989, May. 60(5): 248-254.
49. Almukhtar A, Ju X, Khambay B, McDonald J, Ayoub A (2014) Comparison of the Accuracy of Voxel Based Registration and Surface Based Registration for 3D Assessment of Surgical Change following Orthognathic Surgery. *PLoS ONE*. 9(4): e93402.

## Figures



**Figure 1:** Photograph of a dried mandible with Play-Doh® soft tissue equivalent material



**Figure 2A**





**Figure 2B**

**Figure 2:** Intraoral radiographs of the same site pre- (2A) and post-defect (2B). Note the bone loss distal to #21 in the post-defect radiograph.



**Figure 3A**



**Figure 3B**

**Figure 3:** Measuring the alveolar bone defect depth (3A) and width of the facial and lingual bone (3B) clinically with a UNC-15 periodontal probe.

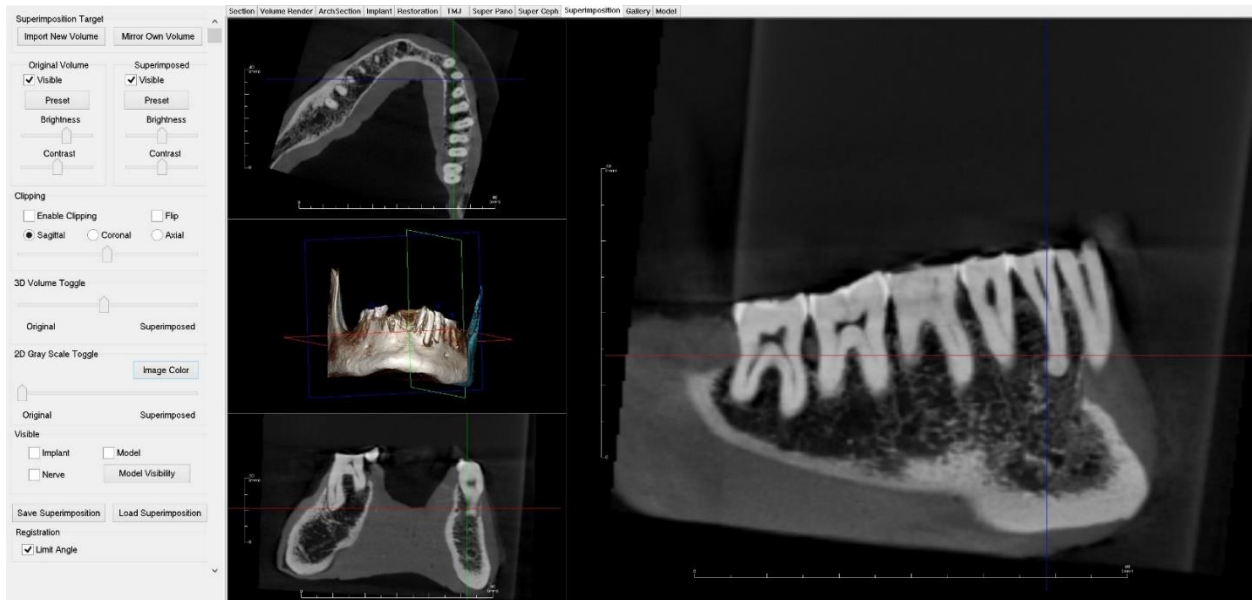


**Figure 4A:** Superimposition window in Anatomage Invivo v. 5.4.5 with registered CBCTs showing the same quadrant without bone defects.

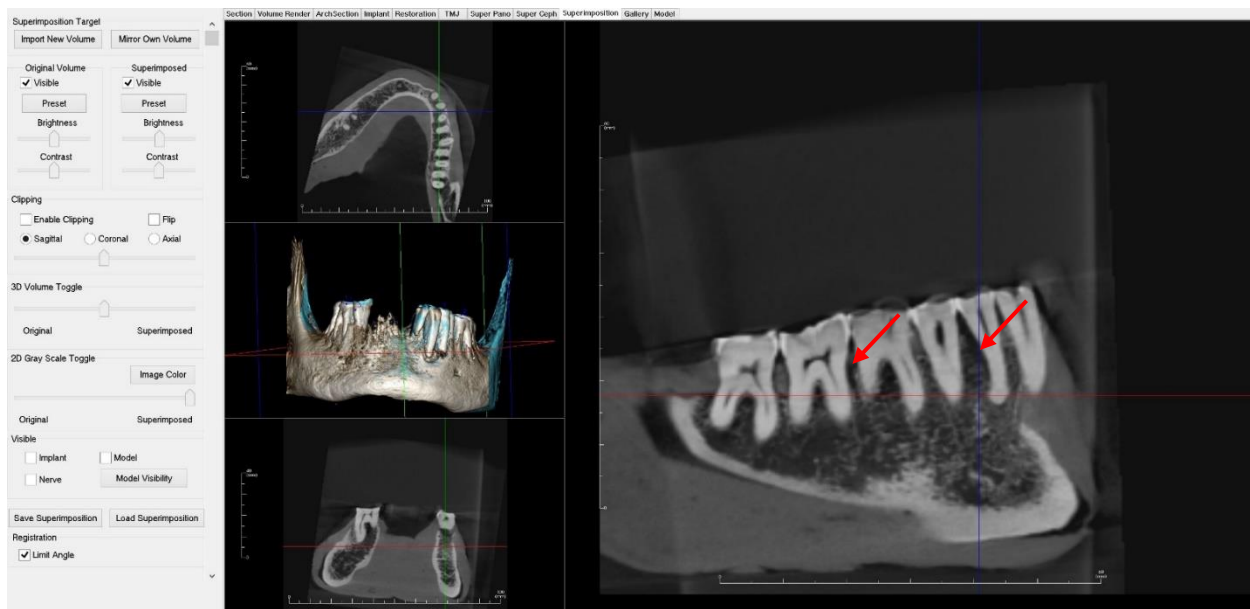


**Figure 4B:** Superimposition window in Anatomage Invivo v. 5.4.5 with registered CBCTs showing the same quadrant with alveolar bone defects (red arrows). Note that in addition to the defect distal to #21, there is a defect mesial to #18 which was not visualized in the two-dimensional radiograph.

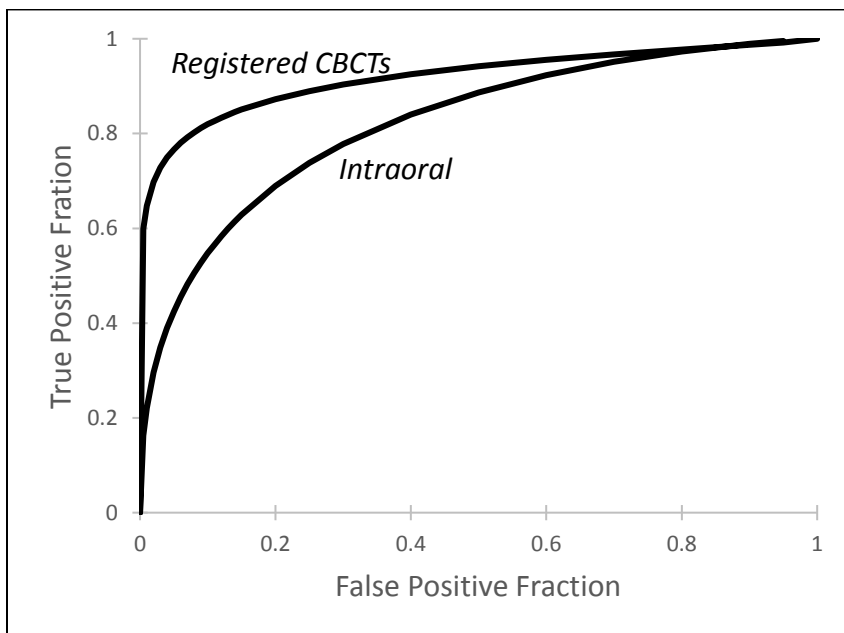


**Figure 5:** ROC curves based on pooled data between registered CBCTs and intraoral radiographs for detection of alveolar bone loss

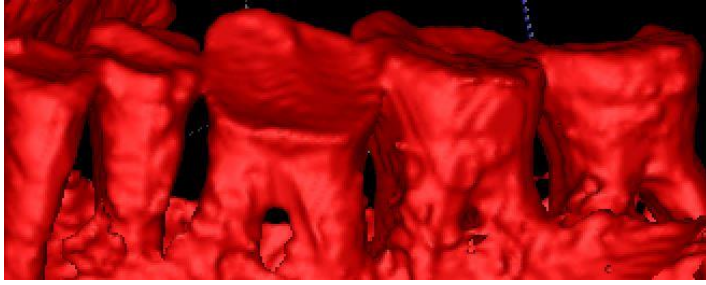


**Figure 6A**

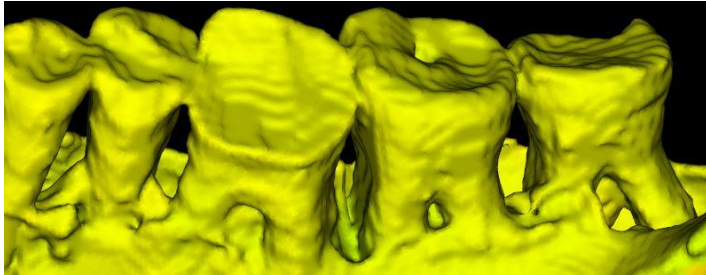


**Figure 6B**

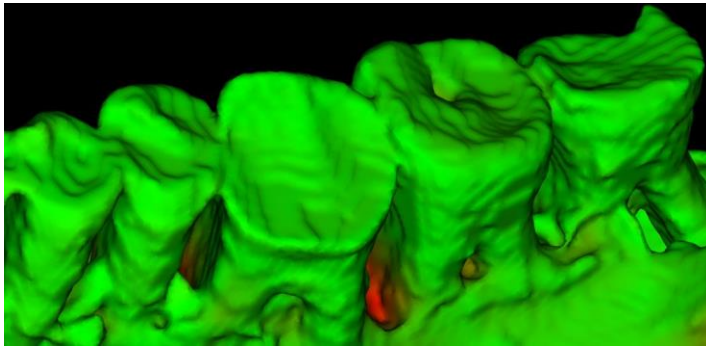


**Figure 6C**

**Figure 6:** Segmented mandibles pre- (5A) and post-defect (5B) in ITK-SNAP combined to show a color map (5C) of the same quadrant in 3D Slicer v. 3.1. Red corresponds to 5 mm bone loss mesial #18.

## Tables

<b>Table 1: Alveolar Bone Defect Ground Truth</b>	
0 mm (no defect)	34
0 - 2.4 mm	0
2.5 - 4.9 mm	11
5 - 7.4 mm	27
7.5 - 10 mm	3
Total	75

<b>Table 2: ROC area under the curve (AUC), sensitivity and specificity based on pooled data</b>			
<b>Imaging Modality</b>	<b>AUC</b>	<b>Sens</b>	<b>Spec</b>
Intraoral	0.81	0.63	0.84
Registered CBCTs	0.90	0.85	0.91

<b>Table 3: Paired t-tests for area under the curve (AUC), sensitivity and specificity between intraoral radiographs and registered CBCTs</b>			
	<b>Mean</b>	<b>Std Dev</b>	<b>Pr &gt;  t </b>
<b>AUC</b>	0.09	0.09	0.06
<b>Sens</b>	0.21	0.12	0.01
<b>Spec</b>	0.07	0.21	0.45

<b>Table 4: Type 3 Analysis of Effects</b>		
<b>Effect</b>	<b>Wald Chi-Square</b>	<b>Pr&gt;ChiSq</b>
Bucco-Lingual Bone Thickness	30.64	<0.0001
Imaging Modality	15.24	<0.0001
Observer	66.27	<0.0001

<b>Table 5: Odds Ratio Estimates</b>			
<b>Effect</b>	<b>Point Estimate</b>	<b>95% Wald Confidence Limits</b>	
CBCT vs. Intraoral Radiographs	2.29	1.51	3.46
Bucco-Lingual Bone Thickness	1.52	1.31	1.77

<b>Table 6: Inter-Observer Reliability (Intraclass Correlation)</b>		
<b>Imaging Modality</b>	<b>Confidence of Detection</b>	<b>Measurement of Extent</b>
<b>Intraoral Radiographs</b>	0.56	0.58
<b>Registered CBCTs</b>	0.59	0.56

<b>Table 7: Weighted Kappa Values for Confidence of Bone Loss Detection</b>								
	<b>Observer</b>	<b>IO_Kappa</b>	<b>IO_95% CI</b>		<b>CBCT_Kappa</b>	<b>CBCT_95% CI</b>		<b>Pr&gt;ChiSq</b>
	1	0.60	0.46	0.74	0.76	0.62	0.90	0.12
	2	0.60	0.46	0.74	0.43	0.23	0.63	0.19
	3	0.51	0.35	0.68	0.56	0.35	0.77	0.72
	4	0.51	0.36	0.66	0.63	0.45	0.81	0.30
	5	0.22	0.03	0.41	0.70	0.55	0.86	0.0001
	6	0.66	0.51	0.82	0.62	0.45	0.80	0.73
<b>Mean</b>		0.52	0.36	0.67	0.62	0.44	0.79	0.35
<b>SD</b>		0.16	0.17	0.14	0.11	0.14	0.09	0.31

<b>Table 8: Weighted Kappa Values for Measurement of Bone Loss Extent</b>								
	<b>Observer</b>	<b>IO_Kappa</b>	<b>IO_95% CI</b>		<b>CBCT_Kappa</b>	<b>CBCT_95% CI</b>		<b>Pr&gt;ChiSq</b>
	1	0.82	0.65	1.00	0.80	0.63	0.98	0.88
	2	0.73	0.57	0.90	0.47	0.21	0.72	0.08
	3	0.59	0.44	0.75	0.48	0.31	0.66	0.37
	4	0.35	0.18	0.52	0.56	0.37	0.75	0.11
	5	0.29	0.08	0.49	0.78	0.66	0.91	<0.0001
	6	0.78	0.64	0.92	0.64	0.42	0.85	0.28
<b>Mean</b>		0.59	0.42	0.76	0.62	0.43	0.81	0.34
<b>SD</b>		0.23	0.24	0.21	0.15	0.18	0.12	0.32

<b>Table 9: Bowker's Test of Symmetry</b>				
	<b>Confidence of Detection Pr&gt;S</b>		<b>Measurement of Extent Pr&gt;S</b>	
<b>Observer</b>	<b>Intraoral</b>	<b>Registered CBCTs</b>	<b>Intraoral</b>	<b>Registered CBCTs</b>
1	0.06	0.88	0.95	0.98
2	0.91	0.65	0.91	0.96
3	0.55	0.42	0.92	0.21
4	0.26	0.93	0.57	0.97
5	0.09	0.41	0.87	0.53
6	0.67	0.22	0.63	0.87

## APPENDIX I

<b>Table 10:</b> Individual ROC area under the curve (AUC), sensitivity and specificity data for each observer and imaging modality							
	<b>Observer</b>	<b>AUC IO</b>	<b>AUC CBCT</b>	<b>Sens IO</b>	<b>Sens CBCT</b>	<b>Spec IO</b>	<b>Spec CBCT</b>
	1	0.82	0.93	0.46	0.88	0.97	0.85
	2	0.77	0.78	0.46	0.55	0.94	0.97
	3	0.84	0.90	0.71	0.93	0.88	0.85
	4	0.87	0.96	0.68	0.88	0.88	0.94
	5	0.69	0.94	0.83	0.93	0.41	0.88
	6	0.91	0.92	0.66	0.90	0.94	0.94
<b>Mean</b>		<b>0.81</b>	<b>0.90</b>	<b>0.63</b>	<b>0.85</b>	<b>0.84</b>	<b>0.91</b>
<b>SD</b>		<b>0.08</b>	<b>0.06</b>	<b>0.15</b>	<b>0.15</b>	<b>0.21</b>	<b>0.05</b>

## APPENDIX II

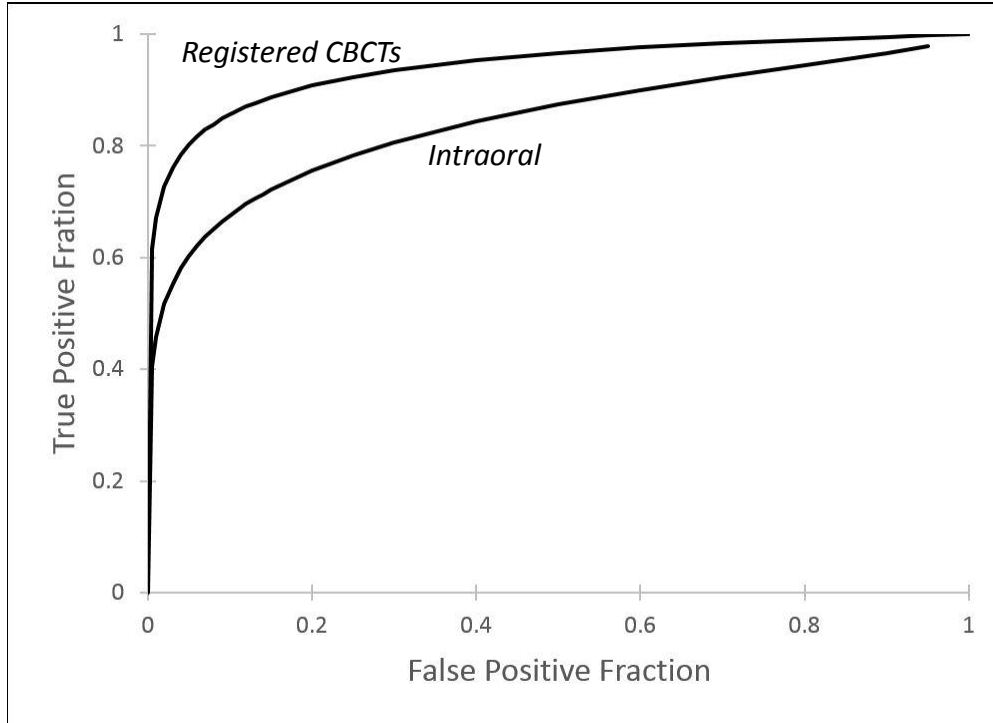


**Figure 7:** ROC curves for Observer 1 for Detection of Alveolar Bone Defects with Intraoral Radiographs and Registered CBCTs

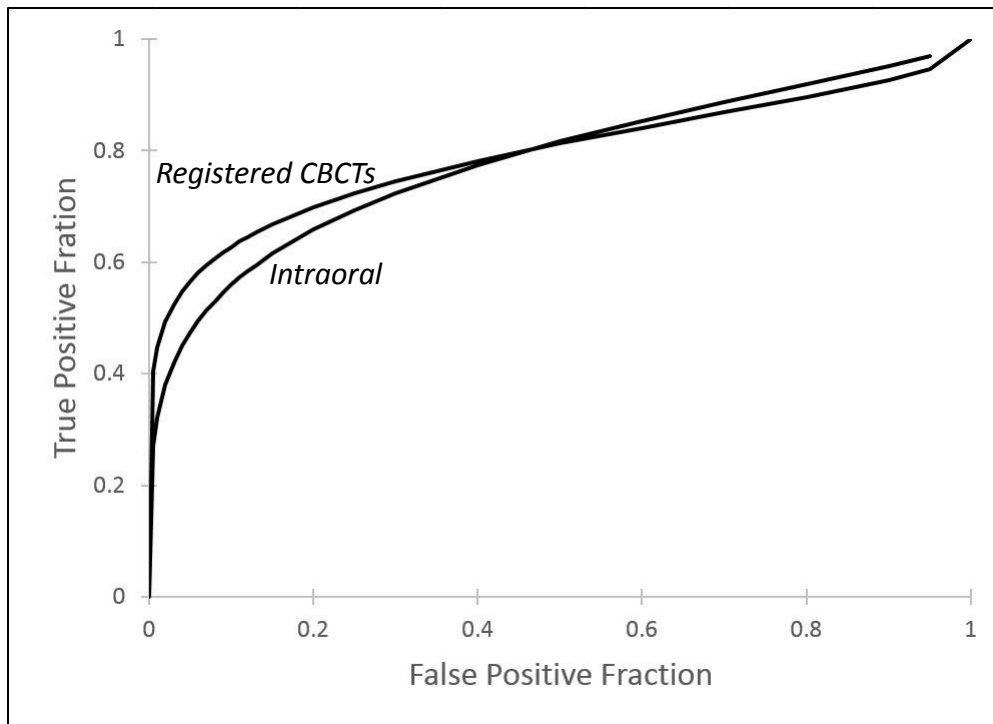


**Figure 8:** ROC curves for Observer 2 for Detection of Alveolar Bone Defects with Intraoral Radiographs and Registered CBCTs



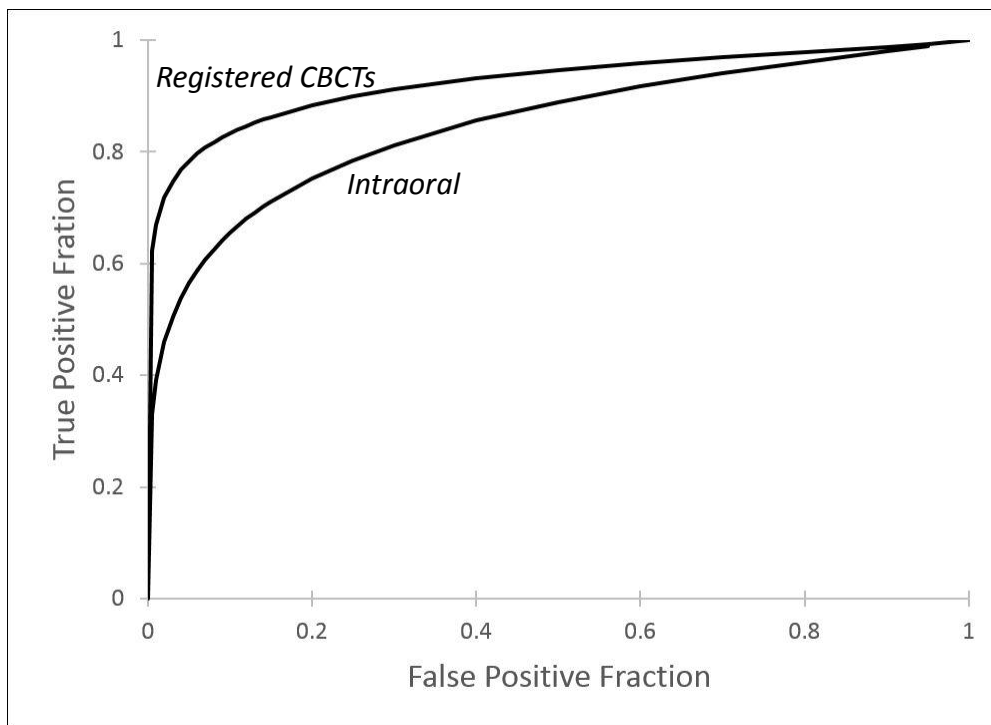


**Figure 9:** ROC curves for Observer 3 for Detection of Alveolar Bone Defects with Intraoral Radiographs and Registered CBCTs

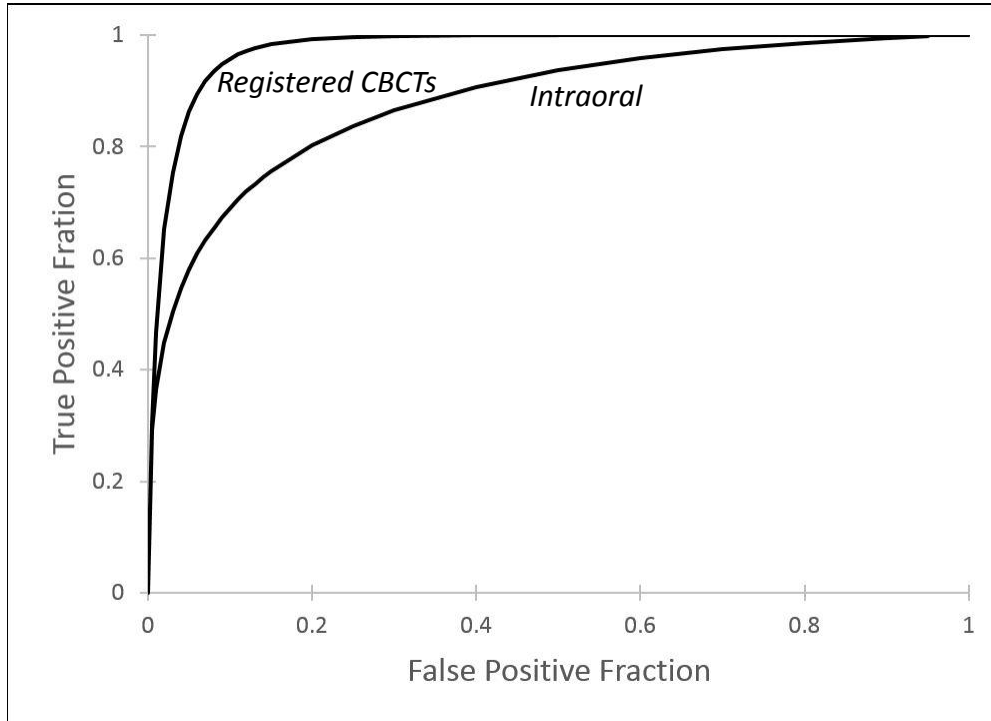


**Figure 10:** ROC curves for Observer 4 for Detection of Alveolar Bone Defects with Intraoral Radiographs and Registered CBCTs

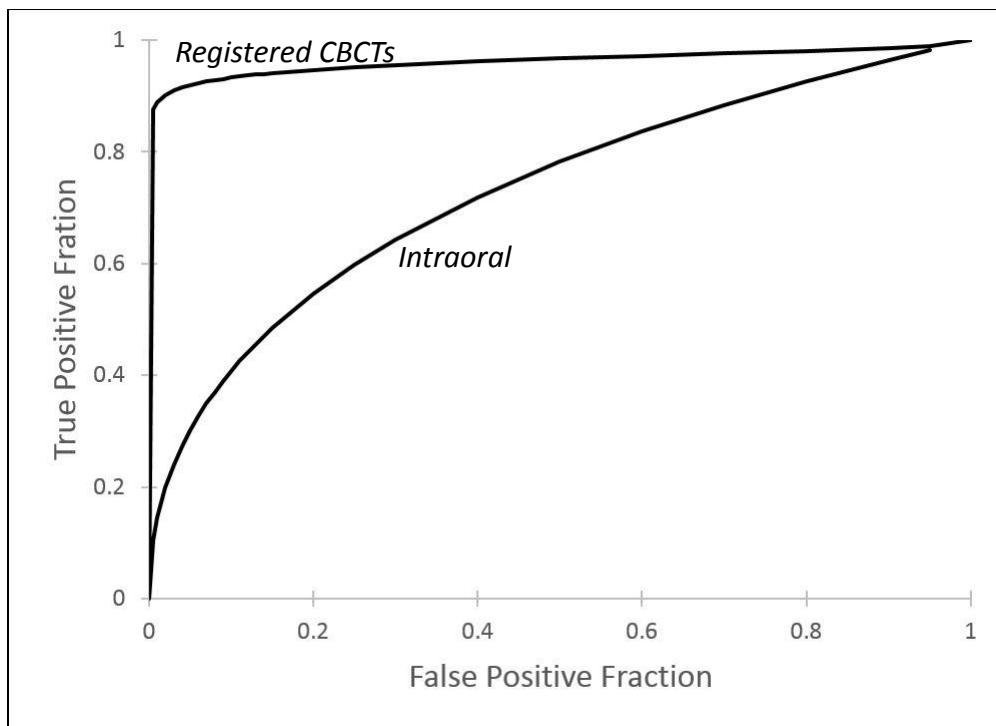


**Figure 11:** ROC curves for Observer 5 for Detection of Alveolar Bone Defects with Intraoral Radiographs and Registered CBCTs

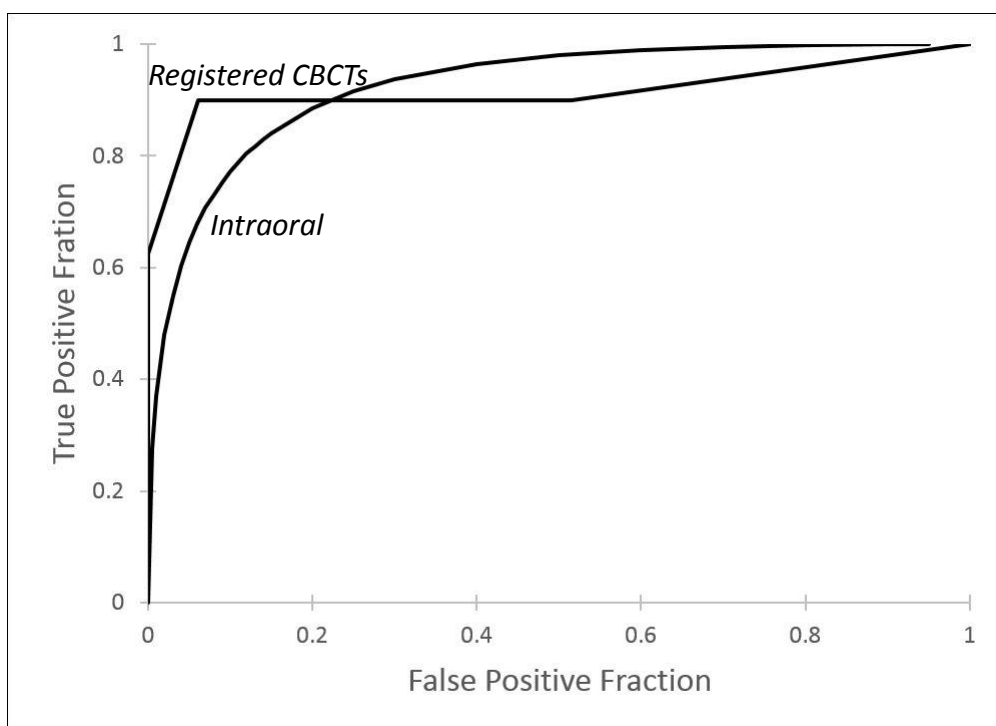


**Figure 12:** ROC curves for Observer 6 for Detection of Alveolar Bone Defects with Intraoral Radiographs and Registered CBCTs